Radiation from Bends in Dielectric Rod Transmission Lines

ERNST-GEORG NEUMANN AND HANS-DIETER RUDOLPH

***Abstract*—The radiation from the fundamental mode propagating around curved dielectric rod transmission lines is investigated experimentally with microwave frequencies. Three methods are used to determine the attenuation by radiation: measuring the insertion loss of bends, measuring the Q-factor of ring resonators, and measuring the Q-factor of sections of curved dielectric rod transmission lines terminated by large reflecting plates.**

The attenuation is found to depend mainly on the combination $R\lambda_0^2/r_0^3$, where R is the radius of curvature, λ_0 the free space wavelength and r_0 a measure of the transverse field extent of the HE_{11} mode. The experimental results are compared with theoretical predictions of other authors. The measured values of the attenuation constant are found to be smaller than the theoretical values.

The distribution of the electromagnetic field near bends is recorded using a semiautomatic field plotter. From the field pictures, it can be concluded that the curved dielectric waveguide radiates tangentially from the outer side. The results presented will also be useful for understanding the mechanism of radiation from bent optical waveguides.

I. INTRODUCTION

DIELECTRIC ROD transmission lines became interesting for communication purposes either in the millimeter wave region [1] or in the optical region in the form of the glass fiber transmission line [2] or the transmission lines for integrated optics [3]. These open lines radiate power from any inhomogeneity, e.g., from a bend.

The calculation of the radiation from a curved dielectric rod transmission line is a complicated task and only recently three approximate theories have been developed [4]–[6]. But the analogous two-dimensional problem of radiation from a curved dielectric slab or a curved reactance plane has been investigated by several authors [5]–[17]. Some of these claimed that their results would also apply for the three-dimensional case.

The radiation from curved dielectric waveguides seems so far to have been studied experimentally only by Kapron and coworkers [18]. They found good agreement with the theory of Marcatili and Miller [15] with regard to the dependence of the bending loss on the radius of curvature. But they did not compare the measured absolute values of the bending loss with available theories.

Therefore and because the various theories looked rather different, we made an experimental investigation of the wave propagation along curved dielectric rod waveguides.

Manuscript received April 12, 1974; revised July 22, 1974.
The authors are with the Institut für Hoch- und Höchstfrequenztechnik, Ruhr-Universität, Bochum, Germany.

II. DEFINITION OF THE QUANTITIES TO BE MEASURED

We consider a dielectric rod with permittivity ϵ surrounded by air. For the straight guide at a frequency $\omega/2\pi$, the phase constant of the fundamental HE_{11} mode will be β and the attenuation constant caused by dielectric losses α_D. The rod is assumed to be so thin that only the HE_{11} mode can be propagated by the rod.

If the dielectric rod transmission line is curved, it still can guide an electromagnetic wave, the field of which near the rod resembling that of the HE_{11} wave on a straight rod. But there will be additional power loss by radiation. The attenuation constant measured along the guide axis is

$$\alpha = \alpha_{DR} + \alpha_R \tag{1}$$

where α_{DR} is the attenuation caused by dielectric losses for the curved rod and α_R is the additional attenuation caused by radiation. The phase constant of the wave propagating along the bent dielectric rod (defined for the rod axis) will differ by $\Delta\beta$ from that of the straight guide:

$$\beta_R = \beta + \Delta\beta. \tag{2}$$

At the beginning of a curved section in an otherwise straight rod, the mode propagating along the straight guide transforms into the mode for the bent guide. As both modes have different transverse field distributions the launching efficiency will be smaller than 100 percent [4], [17]. As we assumed monomode waveguides, power can be lost only by reflection and radiation. The junction between the straight and the bent sections can be looked at as a two-port with zero length with a scattering matrix

$$[S] = \begin{bmatrix} s_{11} & s_{12} \\ s_{21} & s_{22} \end{bmatrix} \tag{3}$$

where, because of reciprocity,

$$s_{12} = s_{21}. \tag{4}$$

At the end of the curved section, the mode for the curved guide will be partially retransformed into that for the straight guide. This junction can also be characterized by the scattering matrix (3), if ports 1 and 2 are interchanged and if only the mode for the curved guide is incident on it. If there is any radiation incident on the junction between the curved and the straight sections, there will be reconversion of radiation into a guided wave on the straight section which superimposes on the wave launched by the mode guided along the curved section.

TABLE I
PROPAGATION PARAMETERS OF A STRAIGHT CIRCULAR DIELECTRIC ROD TRANSMISSION LINE WITH A DIAMETER OF 10 mm, $\epsilon = 2.50$, $\tan\delta = 4\cdot10^{-4}$

f	β/β_o	α_D	r_o/λ_o
7.53 GHz	1.0014	0.006 dB/m	3.0
9.24	1.0126	0.05	1.0
13.92	1.132	0.48	0.3

TABLE II
APPROXIMATED PROPAGATION PARAMETERS OF A RECTANGULAR DIELECTRIC ROD TRANSMISSION LINE WITH A CROSS SECTION OF 9.5 mm × 12 mm, $\epsilon = 2.30$, $\tan\delta = 4\cdot10^{-4}$

f	β/β_o	α_D	r_o/λ_o
6.62 GHz	1.0014	0.006 dB/m	3.0
8.17	1.0126	0.05	1.0
12.71	1.132	0.45	0.3

III. CHARACTERISTICS OF THE DIELECTRIC ROD TRANSMISSION LINES INVESTIGATED

Because it is much easier to calculate the propagation constant and the field distribution for dielectric rod transmission lines with circular cross section than for those with rectangular cross section, we mainly used round polystyrene[1] rods with a diameter of 10 mm. The permittivity and the loss tangent were measured using a cavity perturbation method to be $\epsilon = 2.50 \pm 4$ percent and $\tan\delta = 4\cdot10^{-4} \pm 20$ percent at 9 GHz. The value of ϵ was confirmed by measuring the resonant frequencies of a straight dielectric rod resonator (see Section VI).

The phase constant β and the attenuation constant α_D caused by dielectric losses can be calculated from the known theory of the straight circular dielectric rod transmission line [19], [20]. Table I gives typical values of the wave parameters.

The transverse field distribution of the HE_{11} mode outside the rod can be represented by the modified Hankel functions $K_o(r/r_o)$ and $K_1(r/r_o)$ where r is the distance from the axis and r_o is a measure of the transverse field extent

$$r_o^{-2} = \beta^2 - \beta_o^2. \tag{5}$$

$\beta_0 = 2\pi/\lambda_o$ is the phase constant of a free plane wave in air. As the radiation from a bend is a diffraction problem it is the transverse field extent relative to the free space wavelength which determines mainly the losses by radiation [21]. Therefore, we will plot our results as functions of r_o/λ_o where r_o is defined for the straight rod.

Applying bending forces, we could achieve minimum radii of curvature of the rod axis of about 80 cm without breaking the rods. Though applying heat, it turned out to be difficult to get rods with smaller radii of curvature. Therefore, for curved dielectric rods with radii of curvature smaller than 1 m, we used rods with rectangular cross section (9.5 mm × 12 mm or 10 mm × 12 mm) which were cut from polyethylene plates. The permittivity and the loss tangent were measured to be $\epsilon = 2.30 \pm 4$ percent and $\tan\delta = 4\cdot10^{-4} \pm 20$ percent at 9 GHz. Schlösser [22], [23] showed that it is possible to determine the phase constant of a rectangular rod by approximating it by the phase constant of a circular rod of equal cross-sectional area. By this method and also approximating the attenuation constant of the rectangular rod (9.5 mm × 12 mm) by that of the equivalent circular rod (diameter 12 mm) we found the values summarized in Table II.

Goell [24] showed that the field distribution in a cross section of a rectangular dielectric rod transmission line of an aspect ratio near unity is very similar to that of a circular dielectric waveguide. We therefore suppose to get nearly the same results for circular and rectangular dielectric rod transmission lines provided that r_o/λ_o is the same for both waveguides.

IV. FIELD DISTRIBUTION MEASURED AT CURVED DIELECTRIC ROD TRANSMISSION LINES

Before measuring the characteristics α_R, $\Delta\beta$ of curved dielectric rod transmission lines and the scattering matrix [S] of junctions, we tried to get a clearer idea of the wave propagation around bends by recording the field distribution. Using a semiautomatic field plotter [25] we recorded some lines of constant magnitude and constant phase angle of the main component of the electric field. The electric field was polarized normal to the plane of curvature.

The probe used was a small dipole antenna formed by the protruding inner conductor of a miniature coaxial cable and a choke sleeve on the outer conductor. By registering the transverse field distribution of the HE_{11} mode at a straight circular dielectric rod and comparing it with the calculated distribution we found that the distortion of the field by the probe was negligibly small.

Figs. 1–3 show typical field pictures for a 180°-bend and for a closed ring. The probe antenna measured the field in the plane of curvature. The lines of constant magnitude are represented by solid lines and the lines of constant phase angle, i.e., the wavefronts, by dashed lines. Between adjoining lines the field level changes by 5 dB and the phase angle changes by 360°. It can be shown [26] that in the plane chosen and for the field component measured the time average of Poynting's vector is approximately normal to the wavefronts.

In Fig. 1 the fundamental mode is incident along the upper straight section from the left-hand side. For the straight guide the field is symmetrical to the axis. The field strength decays approximately exponentially in the transverse direction, therefore, for a pure traveling wave,

[1] Stycast 0005, Emerson and Cuming, Inc.

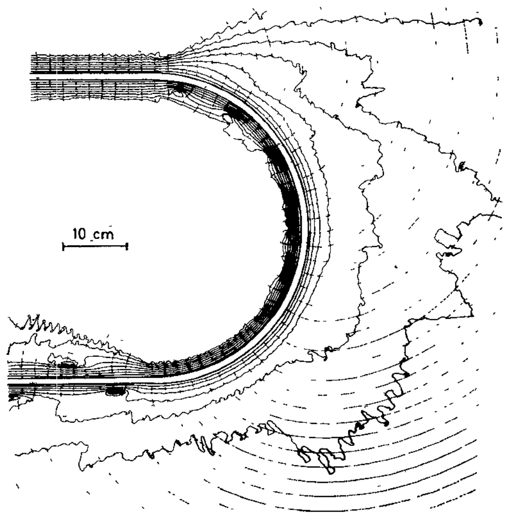

Fig. 1. Lines of constant magnitude (——) and constant phase angle (- - - -) of the electric field measured around an H-plane 180° bend in a dielectric rod transmission line with rectangular cross section of 9.5 mm × 12 mm. Permittivity $\epsilon = 2.30$. Radius of curvature $R = 24.8$ cm. Frequency $f = 12.71$ GHz. Normalized transverse field extent $r_o/\lambda_o = 0.3$.

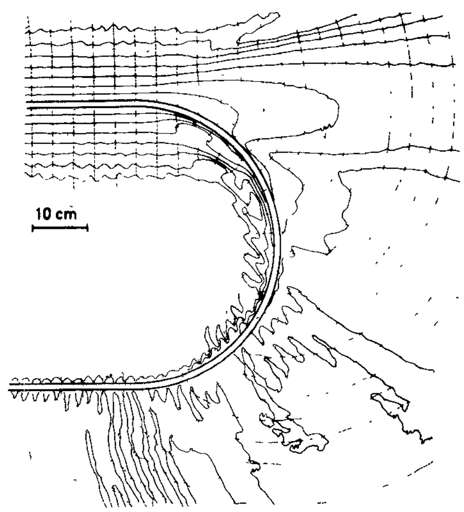

Fig. 2. Electric field distribution measured around a 180° H-plane bend. Cross section 9.5 mm × 12 mm. $\epsilon = 2.30$. $R = 24.8$ cm. $= 8.17$ GHz. $r_o/\lambda_o = 1.0$.

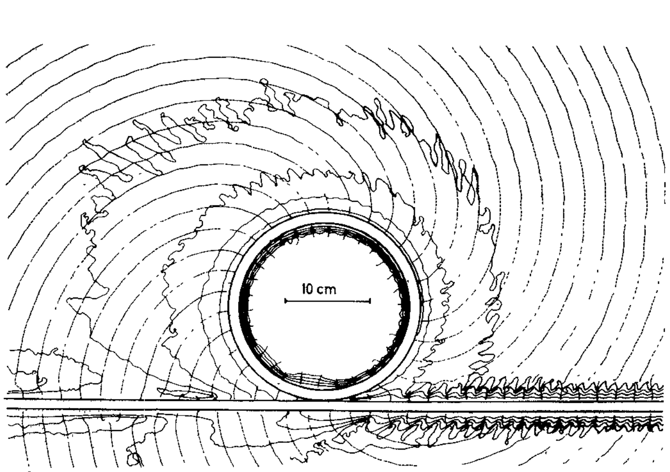

Fig. 3. Electric field distribution measured in the H-plane of a dielectric ring resonator. Cross section 10 mm × 12 mm. $\epsilon = 2.30$. $R = 10.4$ cm. $f = 12.213$ GHz. $r_o/\lambda_o = 0.305$. Critical coupling.

the lines of constant magnitude are straight lines parallel to the guide with the distances between adjoining lines being almost constant. As the lines of constant field magnitude are found to be nearly straight lines, it can be concluded that the element $|s_{11}|$ of the scattering matrix (3) of the junction is very small as compared to unity. As the attenuation by dielectric losses is very small, the average power is flowing in the axial direction and therefore the wavefronts are planes normal to the guide axis. The distance between neighboring wavefronts equals the wavelength of the guided wave.

Behind the junction between the straight and the curved sections, there is some field disturbance because the fields of the guided mode launched on the curved guide and the radiation from the junction superimpose. But for angles greater than about 60°, the field of the wave guided by the bent rod prevails, as can be seen from the fact that the field distribution is the same for each cross section apart from a factor describing the attenuation and the phase retardation. Therefore, one can speak of a "mode" propagating along the bend though its field extends to infinity. The field distribution is no longer symmetrical. On the inner side of the bend the distances between the lines of constant magnitude are smaller than at the straight guide. Therefore, the field decreases more rapidly. On the outer side of the bend the distances are larger than for the straight guide indicating a slower field decay. On the outer side the field extends to infinity showing that part of the power guided is transformed into radiation. Near the curved guide the wavefronts are planes almost normal to the local direction of the axis. But on the outer side of the bend beyond a certain critical distance x_{cr} (see (12)) from the axis they become curved. Applying the theorem for the direction of Poynting's vector, one sees that power is radiated tangentially from the outer side of the bend.

At the end of the curved section most of the power of the mode at the curved guide is retransformed into the fundamental mode of the straight rod. For a short distance behind the junction, the field of the guided wave is disturbed by the superimposed radiation from the curved section and from the junction.

The total insertion loss of the bend of Fig. 1 was 0.5 dB. Subtracting the attenuation by dielectric losses (0.4 dB), one gets for the attenuation by radiation from the bend and both junctions only 0.1 dB. Therefore, one can say that the wave is tightly bound to the waveguide. The transverse field extent was $r_o = 0.3\lambda_o$. Though only 2.3 percent of the power was lost by radiation, the radiation field can clearly be seen. Plotting the field near a bend (or any other inhomogeneity) is therefore a very sensitive method to detect power loss by radiation.

The radiation loss depends critically on frequency. This can be seen from Fig. 2 where, for the same bend as in Fig. 1, the frequency was 8.17 instead of 12.71 GHz. The transverse field extent of the wave at the straight guide is larger ($r_o = \lambda_o$) than in Fig. 1 as can be seen from the greater distances between neighboring lines of constant amplitude. The wave propagating along the curved section is strongly attenuated by radiation. The total insertion loss of the 180° bend exceeds 40 dB. Fig. 2 therefore shows the behavior of a wave loosely bound to the waveguide.

Finally, Fig. 3 shows the field around a ring resonator which is critically coupled to a straight dielectric rod transmission line. In this case the primary wave is incident from the right-hand side. Because the wave radiated tangentially from the ring penetrates the field of the primary wave the lines of constant magnitude at the straight guide are no longer straight lines. The frequency $f_n = 12.213$ GHz was chosen to be a resonant frequency of the ring (diameter of the rod axis $2R = 20.8$ cm), so that the circumference of the ring equalled 30 wavelengths. For a cross section of 10 mm $\times$ 12 mm and a permittivity $\epsilon = 2.30$, the quantity r_o for the straight guide would be $0.305\lambda_o$. The loaded Q-factor of the critically coupled ring resonator was measured to be $Q_L = 15.6$. From this figure the attenuation of the wave for one complete round trip can be calculated (see (19)) to be $\alpha \cdot 2\pi R \cdot 20 \cdot \log(e) = 9.6$ dB. This value is consistent with the form of the lines of constant magnitude in Fig. 3.

V. FIELD DISTRIBUTION CALCULATED FOR A CURVED SLAB WAVEGUIDE

For comparison, we calculated the field distribution of the fundamental TE-wave circulating azimuthally (in the φ-direction) around a hollow lossless dielectric cylinder with radii b and $a > b$. Outside the cylinder the component of the electric field parallel to the axis of the cylinder is proportional to [12], [16]

$$E_z \sim H_\nu^{(2)}(\beta_o \rho) \exp(-j\nu\varphi) \qquad \text{for } \rho > a \tag{6}$$

and inside the cylinder it is proportional to

$$E_z \sim J_\nu(\beta_o \rho) \exp(-j\nu\varphi) \qquad \text{for } \rho < b. \tag{7}$$

ρ is the distance from the axis of the cylinder. The order ν of the Hankel function $H_\nu^{(2)}$ and of the Bessel function J_ν is the propagation constant $\gamma_R = \alpha_R + j\beta_R$ ($\alpha_{DR} = 0$) measured along the outer surface of the cylinder ($\rho = a$) multiplied by a/j:

$$\nu = -ja\gamma_R = (\beta_R - j\alpha_R)a. \tag{8}$$

As the radius of curvature a is normally large as compared to the wavelength, the magnitude of ν is a large number. Because of the radiation loss ($\alpha_R \neq 0$), ν is a complex quantity. The argument of the functions is of the same order of magnitude as the order ν.

Using known approximations [27] for the Hankel and Bessel functions, we calculated some lines of constant magnitude and constant phase angle of E_z. Fig. 4 shows these lines for the parameters $\beta_R a = 30$, $\beta_o a = 26.61$, $a = 11$ cm, and $\alpha_R a = 0.176$. The last value is equivalent to a round trip attenuation of 9.6 dB. The other values correspond to those of Fig. 3, too.

The vertical straight line in Fig. 4 indicates a radial cut. On the right-hand side of the cut we assumed an exciting field distribution which is identical with that of the fundamental mode on the curved slab waveguide. On the left-hand side of the cut we assumed an infinitely thin absorbing screen by which the wave is absorbed after one round trip.

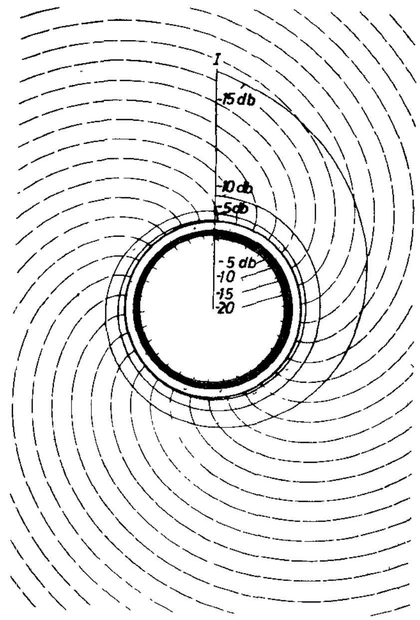

Fig. 4. Electric field distribution calculated around a hollow dielectric cylinder. Outer radius $a = 11$ cm. Inner radius $b = 9.8$ cm. $\beta a = 30$. $\beta_o a = 26.61$. $\alpha_R a = 0.176$. $\alpha_D = 0$.

For large distances $\rho \gg a$ from the cylinder, the wavefronts are Archimedian spirals. The distances between them equal the free space wavelength. Within the cylinder the wavefronts depart only very slightly from radial planes. Because of the attenuation by radiation, the lines of constant field strength are spirals which approach the curved slab.

Comparings Figs. 3 and 4 shows that the field distribution around a curved dielectric rod waveguide is very similar to that around a curved slab waveguide. We found that the wavefronts nearly coincide for both waveguides whereas the lines of constant magnitude differ somewhat. This seems plausible as in the far field we have cylindrical waves for the curved slab whereas we have spherical waves for the curved rod.

With increasing curvature the field distribution becomes more asymmetrical. This can be seen from Fig. 5 where we plotted the magnitude of E_z relative to its values at the surfaces of the curved dielectric slab ($\rho = a$ or $\rho = b$) as a function of the relative distance from the surface $(\rho - a)/\lambda_0$ or $(\rho - b)/\lambda_o$.

The thickness of the plate $a - b$ is assumed to be chosen in such a way that for the straight guide $r_o = 0.3\lambda_o$. For the straight guide ($\beta_o a = \infty$), the field decays symmetrically and exponentially at both sides of the slab

$$E_z \sim \exp(-x/r_o) \tag{9}$$

or

$$E_z \sim \exp(+x/r_o) \tag{10}$$

where x is the coordinate normal to the plane of the slab. With decreasing radius of curvature a at the concave

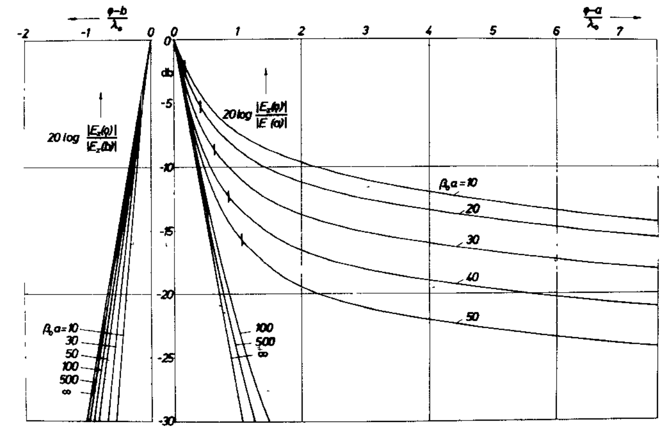

Fig. 5. Magnitude of the electric field of the fundamental wave circulating azimuthally around a hollow dielectric cylinder as a function of the normalized distance from the inner or outer surface. Parameter is the normalized radius of curvature $\beta_o a = 2\pi a/\lambda_o$. The width of the slab, the permittivity, and the frequency have been chosen in such a way that for the straight slab $r_o = 0.3\ \lambda_o$.

side, the slope of the field distribution curve becomes steeper and at the convex side it becomes flatter.

In Fig. 5 by dashes we denoted the distance $\rho_{cr} - a$ from the surface for which

$$\beta_o \rho_{cr} = \beta_R a. \tag{11}$$

This equation means that a hypothetical wave propagating with the velocity of light along a circle of radius ρ_{cr} would suffer the same phase delay as the fundamental mode at the bent slab. For $\rho > \rho_{cr}$, this hypothetical wave would have to travel with a velocity larger than the velocity of light. The critical distance

$$x_{cr} = \rho_{cr} - a = (\beta_R/\beta_o - 1) \cdot a \tag{12}$$

marks the region where the approximately exponential decay of the guided wave changes over into the slow decay of the radiation field and where the radial plane wavefronts of the guided part change over in the curved wavefronts of the radiated part.

VI. METHODS FOR MEASURING THE ATTENUATION BY RADIATION

In order to determine the characteristics of curved dielectric rod transmission lines, we measured the Q-factors of two kinds of resonators incorporating bent dielectric rod transmission lines and the insertion loss of bends [28].

Most of the experimental results were obtained using a resonator which consisted of a section of circular dielectric rod transmission line (length $l \approx 1.2$ m) which at both ends was terminated by large plane metal reflectors (0.5 m × 1.2 m) normal to the local direction of the guide axis. The ends of the rod were placed in small holes in the metal plates. Through these holes of equal diameter, power was coupled from standard rectangular waveguide into the resonator and out of it.

It can be shown [28] that the loaded Q-factor of the resonator is given by

$$Q_L = \frac{f_n}{\Delta f} = \frac{l\omega_n}{2(q + \alpha \cdot l)} \frac{1}{v_g} \tag{13}$$

where Δf is the full half-power width of the transmission curve measured with a matched detector, f_n a resonant frequency, v_g the group velocity, and

$$q = -\ln |s_{22}^R|. \tag{14}$$

For the derivation of (13) we assumed that the attenuation $\alpha \cdot l$ was small and that the magnitude of the reflection factor s_{22}^R of the metal reflectors as seen from the dielectric rod side was approximately unity, i.e., $q \ll 1$.

In order to determine the additional attenuation caused by radiation the loaded Q-factor was measured for the straight rod (Q_{Ls}) and for the same rod curved by mechanical forces (Q_{Lc}). From these values one gets

$$\alpha_R = \frac{1}{2} \frac{\omega_n}{v_g} \left(\frac{1}{Q_{Lc}} - \frac{1}{Q_{Ls}} \right). \tag{15}$$

To derive (15), we assumed the quantities q, v_g, and α_{DR} to be independent on the radius of curvature. The quantity q can be determined from the Q-factors measured for two different lengths of the rod but constant radius of curvature. Within the experimental errors q turned out to be independent on R. Normally, the attenuation α_D caused by dielectric losses is small as compared to the attentuation constant α_R caused by radiation (see Tables I and II). Moreover, for small values of curvature $1/R$, the transverse field distribution at the curved rod will resemble that at the straight rod. Therefore, it seems justified to approximate the value α_{DR} for the curved guide by that (α_D) for the straight guide. From the difference in the resonance frequencies measured for the same rod one time straight and the other time curved (see Fig. 8), one can estimate that for the parameters used in our experiments the relative change in group velocity was always smaller than 1.6 percent.

The experimental errors of α_R determined by this first resonator method were estimated to be smaller than 7 percent.

The second method consisted in measuring the insertion loss of bends using traveling waves. The total insertion loss for a bend of angle θ in an otherwise straight dielectric rod transmission line is given by

$$a_t = -20 \log |s_{21}| + 20 \log (e) (\alpha_{DR} + \alpha_R) R\theta - 20 \log |s_{21}| \tag{16}$$

where we assumed that $|s_{11}| \ll 1$ and $|s_{22}| \ll 1$. By measuring the insertion losses a_{t1} and a_{t2} for two different angles θ_1 and θ_2 for the same R, one can separate the losses by continuous radiation from the losses lumped at the two transitions from the straight to the curved guide and vice versa:

$$\alpha_R = \frac{a_{t2} - a_{t1}}{\theta_2 - \theta_1} \cdot \frac{1}{R\, 20 \log (e)} - \alpha_{DR} \tag{17}$$

and

$$-20 \log | s_{21} | = \frac{1}{2} \frac{\theta_2 \cdot a_{t1} - \theta_1 \cdot a_{t2}}{\theta_2 - \theta_1}. \quad (18)$$

The straight rod in front of the bend had a length of 7 m, that behind the bend a length of 1.3 m. The HE_{11} mode on the straight guide was launched by a circular horn which was surrounded by microwave absorbers in order to absorb most of the free radiation originating at the launcher.

We determined the total insertion loss by terminating the straight line behind the bend by an absorber and measuring the field amplitude at the straight guides in front of and behind the bend. By a newly developed field probe [29], it was possible to achieve a definite coupling between the waveguide and the probe. For α_{DR} we used the value α_D for the straight rod.

The attenuation by power loss at a junction, i.e., $-20 \log | s_{21} |$, was found to be much smaller than the attenuation $20 \log (e) \alpha_R R \pi/2$ by continuous radiation loss along a bend of 90° angle.

The third measuring method consisted in coupling a ring of dielectric waveguide (rectangular cross section 10 mm × 12 mm, $\epsilon = 2.30$) to a straight dielectric rod of the same type. The ring was hanging on thin nylon threads below the straight rod. The coupling could simply be changed by varying the distance between the straight and the bent rod.

The section of coupled waveguides forms a lossless directional coupler [30]. Analysis of the microwave network consisting of the directional coupler and the ring transmission line gave, for critical coupling and assuming $\alpha \cdot 2 \cdot \pi \cdot R \ll 1$, [28]

$$\alpha 4 \pi R = \ln \left(1 + \pi \frac{v_p}{v_g} \frac{n}{Q_L} \right) \quad (19)$$

with

$$n = \beta_R R \quad (20)$$

being the integer number of wavelengths lying at resonance on the circumference of the ring resonator and Q_L its loaded Q-factor. $v_p = \omega/\beta_R$ is the phase velocity.

By sampling the amplitude of the wave circulating around the ring with a small antenna the half power width Δf and the loaded Q-factor $Q_L = f_n/\Delta f$ could be determined. In order to calculate the attenuation constant using (19) we approximated the ratio v_p/v_g of the bent rectangular guide by that for the equivalent straight circular guide of equal cross section.

VII. COMPARISON OF THE ATTENUATION MEASURED WITH THEORETICAL PREDICTIONS

Fig. 6 summarizes the results found with the three methods described in Section VI. The attenuation by continuous radiation from a 90° bend, that means

$$a_R = 20 \log (e) \alpha_R R \pi/2 \quad (21)$$

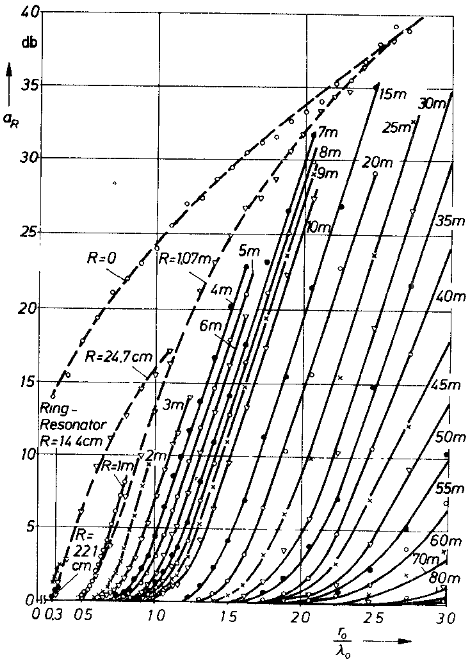

Fig. 6. Attenuation by continuous radiation for a 90°-bend $a_R = 20 \log(e)\alpha_R R\pi/2$ as a function of the normalized transverse field extent r_o/λ_o measured using three different methods. Curve parameter is the radius of curvature R. $R = 0$: insertion loss of a 90° corner (circular rod). R = 14.4 cm and 22.1 cm: ring resonator (rectangular rods). R = 24.7 cm (rectangular rod) and 1.07 m (circular rod): insertion loss. R = 1 m to 100 m: plate resonator (circular rods).

is plotted as a function of r_o/λ_o with the radius of curvature R as a parameter.

The solid lines represent the values measured using the plate-resonator. The curves for R = 24.7 cm and 1.07 m were found by measuring the insertion loss and the curves for R = 22.1 cm and 14.4 cm originated from the ring-resonator method. There is good agreement between the results from the plate resonator and the insertion loss method (R = 1 m and 1.07 m) and the ring resonator method and the insertion loss method (R = 22.1 cm and 24.7 cm). We found no difference in the attenuation constants for the HE_{11} wave polarized normal and parallel to the plane of curvature.

As a limiting case of a 90° bend the uppermost curve in Fig. 6 shows the insertion loss measured for a 90° corner.

At first sight, the formulas for the attenuation constant derived by the different authors [4]–[17] looked very distinct and it seemed difficult to compare them quantitatively with each other and with our measurements. But we found [28] that the formulas could be transformed into similar rather simple forms by assuming that the wave is loosely bound to the waveguide,

$$r_o/\lambda_o \gg 1/(2\pi) \quad (22)$$

that the attenuation constant is small as compared to the phase constant,

$$\alpha_R \ll \beta_R \quad (23)$$

and that the rod radius a is small as compared to the quan-

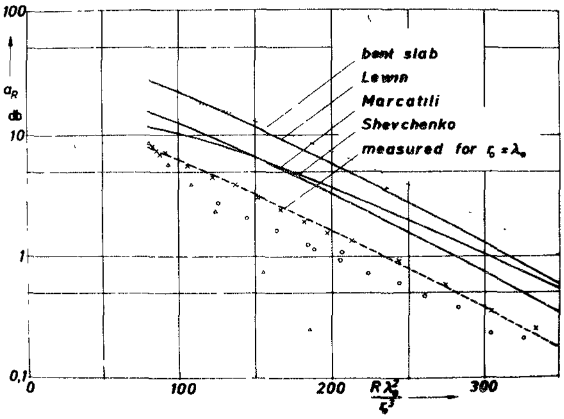

Fig. 7. Attenuation by continuous radiation α_R for a 90° bend as a function of the normalized radius of curvature $R\lambda_o^2/r_o^3$. The crosses represent values measured for $r_o/\lambda_o = 1$ and the dashed curve their average. The solid curves represent formulas (25)–(27) for the bent rod and the dotted curve (28) for the bent slab waveguide. For the circles $r_o/\lambda_o = 0.304\cdots0.355$ and for the triangles $r_o/\lambda_o = 2$.

tity r_o

$$a \ll r_o. \tag{24}$$

Thus [4, eq. (11)] gives

$$\alpha_R \cdot R \approx \frac{\epsilon^{1/2}}{4\pi^2}\frac{R\lambda_o}{r_o^2} \exp\left(-\frac{1}{6\pi^2}\frac{R\lambda_o^2}{r_o^3}\right). \tag{25}$$

Without any approximation [5, eq. (39)] is

$$\alpha_R \cdot R = \frac{1}{2}\left(\frac{R}{r_o}\right)^{1/2} \exp\left(-\frac{1}{6\pi^2}\frac{R\lambda_o^2}{r_o^3}\right). \tag{26}$$

Lewin's formula [6, eq. (8)] can be approximated by

$$\alpha_R \cdot R \approx \frac{1}{2}\left(\frac{R\pi}{r_o}\right)^{1/2} \exp\left(-\frac{1}{6\pi^2}\frac{R\lambda_o^2}{r_o^3}\right). \tag{27}$$

Equations (25)–(27) are for the bent rod. For comparison we also give a formula for the bent slab waveguide:

$$\alpha_R \cdot R \approx \frac{1}{4\pi}\frac{R \cdot \lambda_o}{r_o^2} \exp\left(-\frac{1}{6\pi^2}\frac{R\lambda_o^2}{r_o^3}\right). \tag{28}$$

Equation (28) has been derived by Wait [10] and Logan and Yee [11] and later by Shevchenko [5]. The equations of Miller and Talanov [8, eq. (3.18)], Barlow and Brown [12, eq. (7.40)], and Marcuse [16, eq. (9.6–24)] transform into (28) when using the assumptions (22)–(24). In comparing the various theories we made use of the fact that the attentuation of a curved slab waveguide is only half of that of the corresponding curved reactive surface waveguide [14].

The attenuation is mainly determined by the expression $R\lambda_o^2/r_o^3$ in the argument of the exponential function in (25)–(28). This was supposed by Miller already [31].

In order to compare our experimental results with theoretical predictions, we therefore plotted in Fig. 7 the attenuation α_R of a 90° bend (21) as a function of the normalized radius of curvature $R\lambda_o^2/r_o^3$. The solid lines represent (25)–(27) for the curved rod for the special case $r_o = \lambda_o$, $\epsilon = 2.5$. For comparison, the dotted line represents (28) for the curved slab for $r_o = \lambda_o$, too. The crosses represent measured values extracted from Fig. 6 but omitting those data for which the theories are not valid, i.e., for which $R\lambda_o^2/r_o^3 < 80$. The dashed curve has been fitted to the measured radius of curvature as in (26). The measured attenuation is smaller by a factor of 0.5 than predicted by (26).

For constant normalized radius of curvature, (25)–(28) predict that $\alpha_R R$ is proportional to r_o/λ_o. In order to check this dependence, we also plotted some measured points for other values of r_o/λ_o. The circles in Fig. 7 represent values measured using the ring resonator method. As the radii of the two rings were held constant ($R = 14.4$ cm and 22.1 cm) and the frequency was changed, r_o/λ_o is not the same for all points but changes slightly in the interval from 0.304 to 0.355. For constant normalized radius of curvature, the attenuation is smaller than for $r_o/\lambda_o = 1$, but the reduction of α_R is somewhat smaller than expected from the factor r_o/λ_o in (25)–(28). The small triangles in Fig. 7 represent values measured using the plate resonator for $r_o/\lambda_o = 2$. Incompatibly with (25)–(28) for $R\lambda_o^2/r_o^3 > 100$ the attenuation was found to be smaller than for $r_o/\lambda_o = 1$.

VIII. PHASE CONSTANT OF THE WAVE ON A CURVED DIELECTRIC ROD TRANSMISSION LINE

During bending the rod in the plate resonator from $R = \infty$ to a finite value of R of the radius of curvature we observed a small reduction $\Delta f < 0$ of the resonant frequency. From this frequency shift for constant wavelength one can calculate the change of the phase constant for constant frequency

$$\left.\frac{\Delta\beta}{\beta}\right|_{f=\mathrm{const}} = -\left.\frac{v_p}{v_g}\cdot\frac{\Delta f}{f_n}\right|_{\lambda=\mathrm{const}}. \tag{29}$$

v_p and v_g are the phase and the group velocity for the straight rod.

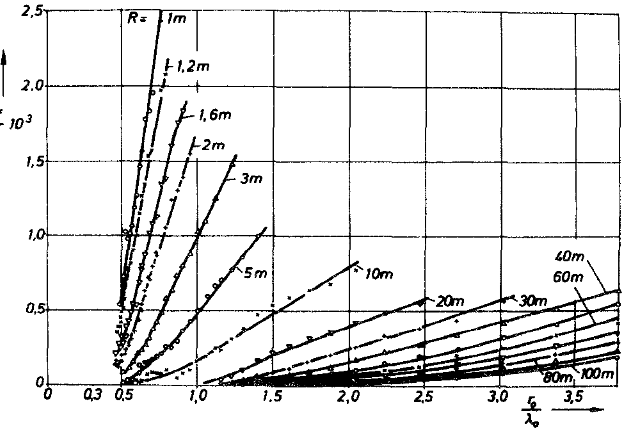

Fig. 8. Relative change of the resonant frequency of the plate resonator by varying the radius of curvature from ∞ to R as a function of r_o/λ_o. Parameter is the radius of curvature.

By bending the rod the phase velocity therefore decreases. This can qualitatively be understood by considering the outward shift of the field maximum with increasing curvature. Assuming that the phase velocity of the maximum remains unchanged, the phase velocity measured along the rod axis will be reduced.

Three authors [10], [12], [17] derived formulas for $\Delta\beta/\beta$ of a bent slab as a function of the radius of curvature and other quantities. In our experiments we found values of $\Delta\beta/\beta$ which were much smaller than those predicted theoretically. For this reason we present in Fig. 8 only our original results for $-\Delta f/f_n$. The polysterene rods had a diameter of 10 mm.

IX. CONCLUSIONS

The attenuation by radiation of the fundamental wave propagating along curved dielectric rod transmission lines has been measured using three different methods at microwave frequencies. The attenuation of a bend of given angle turned out to be determined mainly by the combination $R\lambda_o^2/r_o^3$ of the radius of curvature R, the free space wavelength λ_o, and the transverse field extent r_o of the wave. The attenuation measured was found to be smaller than predicted by several theories.

The field distribution near bends has been measured and represented by lines of constant magnitude and constant phase angle of the electric field strength. From the field pictures, it can be seen that power is radiated tangentially from a bend.

Though the measurements were made at microwave frequencies, it is hoped that the results presented will also give some insight in the behaviour of optical glass fiber waveguides and the waveguides used for integrated optics [32].

REFERENCES

[1] I. A. Ravenscroft and L. A. Jackson, "Proposals for a dielectric rod transmission line," in *Proc. 1973 European Microwave Conf.*, Brüssel, paper B 13,2.

[2] S. E. Miller, E. A. J. Marcatili, and T. Li, "Research toward optical-fiber transmission systems," *Proc. IEEE*, vol. 61, pp. 1703–1751, Dec. 1973.

[3] S. E. Miller, "A survey of integrated optics," *IEEE J. Quantum Electron.* (*Special Issue on 1971 IEEE/OSA Conference on Laser Engineering and Applications, Part II of Two Parts*), vol. QE-8, pp. 199–205, Feb. 1972.

[4] E. A. J. Marcatili, "Bends in optical dielectric guides," *Bell Syst. Tech. J.*, vol. 48, pp. 2103–2132, Sept. 1969.

[5] V. V. Shevchenko, "Radiation losses in bent waveguides for surface waves," *Izv. Vyssh. Ucheb. Zaved. Radiofiz.*, vol. 14, pp. 768–777, 1971.

[6] L. Lewin, "Local form of the radiation condition: Application to curved dielectric structures," *Electron. Lett.*, vol. 9, pp. 468–469, Oct. 1973.

[7] R. S. Elliott, "Azimuthal surface waves on circular cylinders," *J. Appl. Phys.*, vol. 26, pp. 368–376, 1955.

[8] M. A. Miller and V. I. Talanov, "Electromagnetic surface wave guided by a boundary with small curvature," *Zh. Tekh. Fiz.*, vol. 26, pp. 2665–2673, 1956.

[9] V. Vzyatyshev, "Dielektrischeskije wolnowodi," *Sowetskoje Radio*, Moscow, U.S.S.R., 1970.

[10] J. R. Wait, "On the excitation of electromagnetic waves on a curved surface," *IRE Trans. Antennas Propagat.* (Commun.), vol. AP-8, pp. 445–448, July 1960.

[11] N. A. Logan and K. S. Yee, "A simple expression for propagation constants associated with a reactive convex surface," *IRE Trans. Antennas Propagat.* (Commun.), vol. AP-10, p. 103, Jan. 1962.

[12] H. M. Barlow and J. Brown, *Radio Surface Waves.* New York: Oxford, 1962.

[13] S. V. Potter, "Surface wave propagated in azimuth around cylindrical structures, doctoral thesis, University of London, 1963.

[14] G. Böhme, "Die Strahlungsverluste bei der Wellenausbreitung längs gekrümmter dielektrischer Leitungen," *Nachrichtentech.*, vol. 13, pp. 46–49, 1963.

[15] E. A. J. Marcatili and S. E. Miller, "Improved relations describing directional control in electromagnetic wave guidance," *Bell Syst. Tech. J.*, vol. 48, pp. 2161–2188, Sept. 1969.

[16] D. Marcuse, *Light Transmission Optics.* New York: Van Nostrand Reinhold, 1972.

[17] V. V. Shevchenko, "Surface-wave propagation through the bend of a plane guide surface," *Radio Eng. Electron. Phys.*, vol. 8, pp. 1849–1857, 1963.

[18] F. P. Kapron, D. B. Keck, and R. D. Maurer, "Radiation losses in glass optical waveguides," *Appl. Phys. Lett.*, vol. 17, pp. 423–425, 1970.

[19] S. A. Schelkunoff, *Electromagnetic Waves.* New York: Van Nostrand, 1943.

[20] W. M. Elsasser, "Attenuation in a dielectric circular rod," *J. Appl. Phys.*, vol. 20, pp. 1193–1196, 1949.

[21] V. V. Shevchenko, *Continuous Transitions in Open Waveguides.* Boulder, Colo.: Golem Press, 1971.

[22] W. Schlosser, "Der rechteckige dielektrische Draht," *Arch. Elek. Übertragung.*, vol. 18, pp. 403–410, 1964.

[23] ——, "Eine einfache Näherung für das Phasenmaß der Grundwellen am rechteckigen dielektrischen Draht," *Arch. Elek. Übertragung.*, vol. 19, pp. 166–168, 1965.

[24] J. E. Goell, "A circular-harmonic computer analysis of rectangular dielectric waveguides," *Bell Syst. Tech. J.*, vol. 48, pp. 2133–2160, Sept. 1969.

[25] E.-G. Neumann, D. Opielka, and H.-D. Rudolph, "A semiautomatic field plotter," to be published.

[26] E.-G. Neumann and H. D. Rudolph, "Poynting's vector and the wavefronts near a plane conductor," *Electron. Lett.*, vol. 10, pp. 446–447, 1974.

[27] A. Sommerfeld, *Vorlesungen über Theoretische Physik*, vol. IV. Leipzig, Germany: Akademische Verlagsgesellschaft, 1962.

[28] H.-D. Rudolph, "Strahlungsverluste durch Knicke oder Krümmungen in dielektrischen Leitungen," doctoral thesis, University of Bochum, Bochum, Germany, 1974.

[29] E.-G. Neumann, D. Opielka, and H.-D. Rudolph, "A double probe with constant coupling to open waveguides," *Electron. Commun.*, vol. 28, pp. 229–230, 1974.

[30] N. S. Kapany and J. J. Burke, *Optical Waveguides.* New York: Academic, 1972.

[31] S. E. Miller, "Directional control in light-wave guidance," *Bell Syst. Tech. J.*, vol. 43, pp. 1727–1739, 1964.

[32] G. Sinclair, "Theory of models of electromagnetic systems," *Proc. IRE*, vol. 36, pp. 1364–1370, Nov. 1948.